A Hybrid Systems Approach to Dual-Objective Functional Electrical Stimulation Cycling

Saiedeh Akbari, Glen Merritt, Federico M. Zegers, and Christian A. Cousin, *Member, IEEE*

***Abstract*—Motorized functional electrical stimulation (FES) cycling can serve as a physical rehabilitation strategy for individuals whose lower limbs are affected by neurological injuries. Motorized FES cycling is unique among human-robot interaction tasks because the cycle's motor and rider's leg muscles must be simultaneously controlled. In this letter, two tracking objectives are proposed for the combined cycle-rider system. First, the rider's leg muscles are stimulated to pedal the cycle at a desired cadence, and second, the cycle's motor is used to regulate the interaction torque between the cycle and rider using an admittance controller. A novel hybrid systems analysis using Lyapunov- and passivity-based techniques is conducted to prove that the cycle's motor can globally exponentially regulate the admittance error system and prove that the cadence error system is output feedback passive. Experiments conducted on five participants illustrate the efficacy of the controllers with an average admittance error of -0.01±0.70 RPM at an average cadence of 45.51±1.77 RPM for a desired cadence of 50 RPM.**

***Index Terms*—Hybrid systems, Lyapunov, passivity, human-robot interaction, FES, rehabilitation.**

I. Introduction

MILLIONS of people around the world possess some form of neurological injury or disorder including traumatic brain injury, post-stroke hemiparesis, spinal cord injury, or Parkinson's disease [1], [2]. Neurological injuries can impair quality of life (QoL) and make activities of daily living difficult. Such issues may worsen over time due to reduced muscle mass, strength, endurance, and mobility [3]. To prevent QoL degradation, various rehabilitative methods have been investigated including neuromuscular electrical stimulation (NMES). NMES involves the application of an electric field across a muscle to generate muscle contractions [4]. Motorized functional electrical stimulation (FES) cycling is an extension of NMES which can improve mobility and impart numerous health benefits [5]. However, FES cycling is challenged by nonlinear and discontinuous dynamics, time-varying characteristics of muscles, and the need for precise coordination between multiple systems to facilitate cycling objectives [5].

Because motorized FES cycling involves intimate physical human-robot interaction, careful consideration must go into the control design to verify stability and ensure rider safety. Past works by the authors have studied dual-objective control of FES cycling, e.g., [6], [7], from a switched systems perspective, as well as time-varying trajectory generation using external triggers [8] and electromyography [9]. FES cycling may involve competing objectives, e.g., cadence and admittance control, which have been analyzed using Lyapunov- and passivity-based tools using switched systems theory [6]–[8].

Hybrid systems have been gaining traction in recent years [10]–[13] and have been applied to domains ranging from human-robot interaction [14], [15] to the decentralized control of multi-agent systems [16]. The authors in [14] and [15] examine an upper-limb rehabilitation robot and bipedal locomotion, respectively, using a hybrid automata framework. However, neither [14] nor [15] utilized FES, which renders the study of FES from a hybrid systems standpoint an open research topic. For information on hybrid systems and passivity, see [11] and [12], respectively.

Motivated by [6]–[8], [14], [15], we employ the hybrid systems framework of [11] to provide a more thorough, concise, and rich analysis of an FES cycle. To our knowledge, we are the first to study the continuous-time and discrete-time elements of FES cycling under the hybrid systems framework of [11] and the first to apply the more general notion of passivity in [12] to the flow and jump dynamics of an FES cycle. Additionally, we use the hybrid systems paradigm to construct an alternative model of an FES cycle that yields less conservative gain conditions (see [6], [7]) and is robust to vanishing perturbations. For this application of human-robot interaction, we examine two tracking objectives using two sets of actuators for a motorized FES cycle: 1) stimulate the rider's leg muscles to pedal the cycle at a desired cadence, and 2) activate the cycle's motor to regulate the interaction torque between the cycle and rider using an admittance controller. The admittance control objective is recast into a set stabilization problem, where the set of interest is shown to be globally exponentially stable (GES) under certain sufficient conditions determined via a Lyapunov-based stability analysis. Using a passivity-based hybrid systems analysis, we show that the cadence error system is output feedback passive. Moreover, since the hybrid system for the motorized cycle satisfies the

Manuscript received September 14, 2021; revised November 16, 2021; accepted December 8, 2021. Date of publication December 24, 2021; date of current version January 6, 2022. Recommended by Senior Editor C. Prieur. *(Corresponding author: Christian A. Cousin.)*

Saiedeh Akbari, Glen Merritt, and Christian A. Cousin are with the Department of Mechanical Engineering, University of Alabama, Tuscaloosa, AL 35401 USA (e-mail: sakbari@crimson.ua.edu; gmerritt@crimson.ua.edu; cacousin@eng.ua.edu).

Federico M. Zegers is with the Air Force Research Laboratory, Munitions Directorate, Niceville, FL 32542 USA (e-mail: federico.zegers@us.af.mil).

Digital Object Identifier 10.1109/LCSYS.2021.3138190

hybrid basic conditions, and the set of interest is GES, the proposed controller is robust to vanishing perturbations, which can model spasms and volitional contributions. To verify the efficacy of the controllers, experiments were conducted on five participants without any neurological injuries.

II. Preliminaries

A. Notation

Given a set $S \subset \mathbb{R}^n \times \mathbb{R}^m$, we denote the neighborhood of the set as $\Pi(S) \triangleq \{x \in \mathbb{R}^n : \exists_{u \in \mathbb{R}^m}(x,u) \in S\}$. Given a set $S \subset \mathbb{R}^n$, let $\overline{S}$ and con$\{S\}$ denote the closure of S and the convex hull of S, respectively. Given $x, y \in \mathbb{R}_{>0}$, there exist unique integers n, r such that $x = ny + r$. Let x mod y denote the modulo operation, where the remainder $r = x$ mod y. For $x \in \mathbb{R}$ and $\mu \in \mathbb{R}_{>0}$, let $\text{sat}_\mu[x]$ denote a saturation function such that $\text{sat}_\mu[x] \triangleq \mu$ for $x > \mu$, $\text{sat}_\mu[x] \triangleq x$ for $0 \leq x \leq \mu$, and $\text{sat}_\mu[x] \triangleq 0$ for $x < 0$. For $x \in \mathbb{R}$, let $\text{sgn}(x) \triangleq 1$ for $x > 0$, $\text{sgn}(x) \triangleq 0$ for $x = 0$, and $\text{sgn}(x) \triangleq -1$ for $x < 0$.

B. Hybrid Systems

A hybrid system $\mathcal{H}$ with state $\xi \in \mathbb{R}^n$ and data (C, f, D, g) is defined as

$$\mathcal{H} : \begin{cases} \dot{\xi} = f(\xi), & \xi \in C, \\ \xi^+ = g(\xi), & \xi \in D, \end{cases} \tag{1}$$

where $f : \mathbb{R}^n \to \mathbb{R}^n$ denotes the flow map that models continuous behavior, $C \subset \mathbb{R}^n$ denotes the flow set over which the system continuously evolves, $g : \mathbb{R}^n \to \mathbb{R}^n$ denotes the jump map that models discrete behavior, and $D \subset \mathbb{R}^n$ denotes the jump set over which the system discretely evolves. A solution ϕ to the hybrid system $\mathcal{H}$ is parameterized with respect to hybrid-time as denoted by $(t, j) \in \mathbb{R}_{\geq 0} \times \mathbb{Z}_{\geq 0}$. Observe that t denotes continuous time, and j denotes discrete time. The domain dom$\phi \subset \mathbb{R}_{\geq 0} \times \mathbb{Z}_{\geq 0}$ is called a hybrid time domain if for all $(T, J) \in$ domϕ, dom$\phi \cap ([0, T] \times \{0, 1, \ldots, J\})$ can be expressed as $\cup_{j=0}^{J}([t_j, t_{j+1}] \times \{j\})$ for a time sequence $0 = t_0 \leq t_1 \leq \cdots \leq t_{J+1}$. Note that t_j indicates the jth instance the state ξ jumps. A solution ϕ to $\mathcal{H}$ is called maximal if ϕ cannot be extended, that is, ϕ is not a truncated version of another solution. A solution is called complete if its domain is unbounded. The set $\mathcal{S}_\mathcal{H}$ contains all maximal solutions to $\mathcal{H}$, where the set $\mathcal{S}_\mathcal{H}(\xi)$ contains all maximal solutions to $\mathcal{H}$ from ξ. The hybrid system $\mathcal{H}$ with data (C, f, D, g) is said to satisfy the hybrid basic conditions if it satisfies the conditions in [11, Assumption 6.5].

Definition 1 (Global Exponential Stability [10]): Let a hybrid system $\mathcal{H}$ be defined on $\mathbb{R}^n$. Let $\mathcal{A} \subset \mathbb{R}^n$ be closed. The set $\mathcal{A}$ is said to be globally exponentially stable (GES) for $\mathcal{H}$ if there exist $\kappa_1, \kappa_2 > 0$ such that every maximal solution ϕ to $\mathcal{H}$ is complete and satisfies

$$|\phi(t,j)|_\mathcal{A} \leq \kappa_1 \exp(-\kappa_2(t+j))|\phi(0,0)|_\mathcal{A},$$

where $|\phi(t,j)|_\mathcal{A} \triangleq \inf_{y \in \mathcal{A}} |\phi(t,j) - y|$ for each $(t,j) \in$ domϕ.

Definition 2 (Output Feedback Passive): Let $\mathcal{A} \subset \mathbb{R}^n$ be a closed set for a hybrid system $\mathcal{H}$. Let $u_c \in \mathbb{R}^{m_c}$, $u_d \in \mathbb{R}^{m_d}$ denote the inputs acting on the flow and jump dynamics of $\mathcal{H}$, respectively, and let $y_c \in \mathbb{R}^{m_c}$, $y_d \in \mathbb{R}^{m_d}$ denote the outputs of the flow and jump dynamics, respectively. Based on [12, Definition 2] and [17, Definition 6.3], suppose there exists a continuous storage function $V : \mathbb{R}^n \to \mathbb{R}_{\geq 0}$ that is continuously differentiable on some neighborhood of $\Pi(\overline{C})$. The hybrid system $\mathcal{H}$ is said to be output feedback passive with respect to $\mathcal{A}$ whenever

$$\langle \nabla V(\xi), f(\xi, u_c) \rangle \leq u_c^\top y_c + y_c^\top \rho_c(y_c), \ (\xi, u_c) \in C \times \mathbb{R}^{m_c},$$
$$V(g(\xi, u_d)) - V(\xi) \leq u_d^\top y_d + y_d^\top \rho_d(y_d), \ (\xi, u_d) \in C \times \mathbb{R}^{m_d},$$

for some functions $\rho_c : \mathbb{R}^{m_c} \to \mathbb{R}^{m_c}$ and $\rho_d : \mathbb{R}^{m_d} \to \mathbb{R}^{m_d}$.

III. Dynamics

A. Human-Rider Model

According to [18], the dynamic model of the human-rider subsystem can be represented as[1]

$$M_h(q)\ddot{q} + H_h(q, \dot{q})\dot{q} + G_h(q) + P(q, \dot{q}) = \tau_{int}(t) + \tau_h(q, \dot{q}, t), \tag{2}$$

where $t_0 \in \mathbb{R}_{\geq 0}$, $q : \mathbb{R}_{\geq t_0} \to \mathbb{R}$, $\dot{q} : \mathbb{R}_{\geq t_0} \to \mathbb{R}$, and $\ddot{q} : \mathbb{R}_{\geq t_0} \to \mathbb{R}$ denote the initial time, the measurable crank angle of the cycle, the measurable angular velocity of the crank (i.e., cadence), and the unknown angular acceleration, respectively. The inertial, centripetal-Coriolis, and gravitational components of the rider are denoted by $M_h : \mathbb{R} \to \mathbb{R}$, $H_h : \mathbb{R}^2 \to \mathbb{R}$, and $G_h : \mathbb{R} \to \mathbb{R}$, respectively. The rider's passive viscoelastic tissue torques are denoted by $P : \mathbb{R}^2 \to \mathbb{R}$, and the measurable and bounded [19] interaction torque between the rider and cycle is denoted by $\tau_{int} : \mathbb{R}_{\geq t_0} \to \mathbb{R}$. In (2), the torque generated from the rider's muscles (i.e., the right and left quadriceps femoris, hamstrings, and gluteals) is denoted by $\tau_h : \mathbb{R}^2 \times \mathbb{R}_{\geq t_0} \to \mathbb{R}$ such that

$$\tau_h \triangleq B_p u_h, \quad p \in \mathcal{P} \triangleq \{1, 2, \ldots, \mathtt{P}\}, \tag{3}$$

where $\{B_p\}_{p \in \mathcal{P}} \subset \mathbb{R}_{>0}$ denotes a muscle control effectiveness family (i.e., each B_p models a combination of active muscles), $u_h : \mathbb{R}_{\geq t_0} \to \mathbb{R}$ denotes the subsequently defined muscle control input (i.e., the stimulation pulse width), $\mathtt{P} \in \mathbb{N}$ denotes the total number of modes, and each mode corresponds to a specific combination of muscle groups that can apply positive torque to the crank. Let $\mathcal{Q} \triangleq [0, 2\pi)$ and $q^* : \mathbb{R} \to \mathcal{Q}$ denote a wrapped crank angle such that $q^* \triangleq q$ mod 2π. Hence, q^* takes a real-valued angle q and wraps it (i.e., q is mapped between 0 and 2π), where $\mathcal{Q}$ is the co-domain of q^*. Because the effective region of each muscle about the crank changes as a function of the crank angle, let $\mathcal{Q}^* \triangleq \{q_1, q_2, \ldots, q_\mathtt{P}\} \subset \mathcal{Q}$ denote the set of points that elicit a change in the control effectiveness B_p. Note, when no muscles can contribute positive torque about the crank, $B_p = 0$ for some $p \in \mathcal{P}$.

B. Motorized Cycle Model

According to [18], the subsystem dynamics of the cycle can be represented as

$$M_r(q)\ddot{q} + H_r(q, \dot{q})\dot{q} + G_r(q) + b\dot{q} = -\tau_{int}(t) + \tau_r(t), \tag{4}$$

where the cycle's inertial, centripetal-Coriolis, and gravitational effects are denoted by $M_r : \mathbb{R} \to \mathbb{R}$, $H_r : \mathbb{R}^2 \to \mathbb{R}$, and

[1]For notational brevity, all explicit dependence on time, t, within the states $q(t), \dot{q}(t), \ddot{q}(t)$, and all functional dependencies are suppressed unless required for clarity of exposition.

$G_r : \mathbb{R} \to \mathbb{R}$, respectively. The viscous friction is denoted by $b : \mathbb{R}_{>0} \to \mathbb{R}$, and the measurable interaction torque is equal and opposite to τ_{int} in the right-hand side of (2). The torque applied about the crank axis by the cycle's electric motor is denoted by $\tau_r : \mathbb{R}_{\geq t_0} \to \mathbb{R}$ such that

$$\tau_r \triangleq B_r u_r, \tag{5}$$

where $B_r \in \mathbb{R}_{>0}$ and $u_r : \mathbb{R}_{\geq t_0} \to \mathbb{R}$ denote the known motor control constant and the subsequently defined control input to the motor (i.e., the motor current), respectively. To facilitate the analysis, the following properties are provided for the systems in (2) and (4).

Property 1: For $x \in \{h, r\}$, the functions M_x, H_x, G_x, P, and b can be bounded as $c_{m_x} \leq M_x \leq c_{M_x}$, $|H_x| \leq c_{H_x}|\dot{q}|$, $|G_x| \leq c_{G_x}$, $|P| \leq c_{P1} + c_{P2}|\dot{q}|$, and $b \leq c_b$, respectively, where $c_{m_x}, c_{M_x}, c_{H_x}, c_{G_x}, c_{P1}, c_{P2}, c_b \in \mathbb{R}_{>0}$ are known constants [18].

Property 2: For $x \in \{h, r\}$, the inertia and centripetal-Coriolis terms are skew-symmetric, i.e., $\dot{M}_x - 2H_x = \mathbf{0}$ [20].

IV. Control Development

Two tracking objectives are proposed. First, the human-rider in (2) is tasked with tracking a desired cadence. Second, the motorized cycle in (4) is tasked with regulating the interaction torque between the cycle and rider using an admittance filter and controller. To actuate the combined system and examine the stability of the two tracking objectives, two error systems, two controllers, and two hybrid systems are developed.

A. Error System Development

The first error system, referred to as the *cadence error system*, is denoted by $z : \mathbb{R}_{\geq t_0} \to \mathbb{R}^2$ and given as $z \triangleq [e, r]^\top$, where $e : \mathbb{R}_{\geq t_0} \to \mathbb{R}$ denotes a position tracking error and $r : \mathbb{R}_{\geq t_0} \to \mathbb{R}$ denotes a filtered tracking error. The errors are

$$e \triangleq q_d - q, \tag{6}$$

$$r \triangleq \dot{e} + \alpha e, \tag{7}$$

where $q_d : \mathbb{R}_{\geq t_0} \to \mathbb{R}$ denotes a twice differentiable desired position trajectory, and $\alpha \in \mathbb{R}_{>0}$ denotes a selectable control gain. The second error system, referred to as the *admittance error system*, is denoted by $\zeta : \mathbb{R}_{\geq t_0} \to \mathbb{R}^2$ and given by $\zeta \triangleq [\upsilon, \psi]^\top$, where $\upsilon : \mathbb{R}_{\geq t_0} \to \mathbb{R}$ denotes an admitted position tracking error, and $\psi : \mathbb{R}_{\geq t_0} \to \mathbb{R}$ denotes a filtered tracking error. The two errors are

$$\upsilon \triangleq q_a + q_d - q, \tag{8}$$

$$\psi \triangleq \dot{\upsilon} + \beta \upsilon, \tag{9}$$

where $q_a : \mathbb{R}_{\geq t_0} \to \mathbb{R}$ denotes the differentiable admitted position trajectory (generated online), and $\beta \in \mathbb{R}_{>0}$ denotes a selectable control gain. The interaction torque error between the human and cycle is denoted by $e_\tau : \mathbb{R}_{\geq t_0} \to \mathbb{R}$ and

$$e_\tau \triangleq \tau_d - \tau_{int}, \tag{10}$$

where $\tau_d : \mathbb{R}_{\geq t_0} \to \mathbb{R}$ denotes the selectable and differentiable desired interaction torque. To generate the admitted position, q_a, and the admitted cadence, $\dot{q}_a : \mathbb{R}_{\geq t_0} \to \mathbb{R}$, for use in (8) and (9), the interaction torque error is processed using an admittance filter given by

$$e_\tau = M_d \ddot{q}_a + B_d \dot{q}_a, \tag{11}$$

where $\ddot{q}_a : \mathbb{R}_{\geq t_0} \to \mathbb{R}$ denotes the admitted acceleration, the constants $M_d, B_d \in \mathbb{R}_{>0}$ denote selectable filter parameters representing the desired inertia and desired damping of the interaction between the cycle and rider [7], and $q_a(0) = \dot{q}_a(0) = 0$.

B. Cadence Controller

Based on the dynamics in (2), (3), the errors in (6), (7), and the subsequent stability analysis in Section V, the cadence controller used to activate the human-rider's muscles is

$$u_h \triangleq \text{sat}_{U_h}[k_1 r], \tag{12}$$

where $k_1 \in \mathbb{R}_{>0}$ is a selectable control constant, and $U_h \in \mathbb{R}_{\geq 0}$ denotes the maximum allowable stimulation pulse width for the rider's comfort and safety.

C. Admittance Controller

Based on the dynamics in (4), (5), the errors in (8), (9), and the subsequent stability analysis in Section V, the admittance controller is designed as

$$u_r \triangleq B_r^{-1}(k_2 \psi + (1 + \exp(-t))\upsilon + \tau_{int} + \nu \cdot \text{sgn}(\psi)), \tag{13}$$

where $\nu \triangleq k_3 + k_4\|\gamma\| + k_5\|\gamma\|^2$, $k_i \in \mathbb{R}_{>0}$, for each $i = \{2, 3, 4, 5\}$, denotes a constant control gain, B_r is the control effectiveness in (5), and $\gamma : \mathbb{R}_{\geq t_0} \to \mathbb{R}^4$ is a composite vector defined as $\gamma \triangleq [\upsilon, \psi, \dot{q}_a, \ddot{q}_a]^\top \in \mathbb{R}^4$.

D. Human-Rider Hybrid System

Recall, the human-rider is tasked with tracking a desired position and cadence. Let $\tau : \mathbb{R}_{\geq t_0} \to \mathbb{R}_{\geq t_0}$ denote a timer variable that keeps track of time from the desired initial condition, $\tau(t_0) = t_0$, and evolves according to the continuous-time process $\dot{\tau} = 1$ [11]. In addition, let $h_1 : \mathbb{R}^2 \to \mathbb{R} : (q, \dot{q}) \mapsto q + 0.1\dot{q}$ denote an advanced crank angle used to account for the electromechanical delay in a stimulated muscle (approximated as 100 ms and assumed to be constant) [21]. Using (6), (7), and the timer τ, the advanced crank angle can be written in terms of e, r, and τ as $h_1(e, r, \tau) = q_d(\tau) - e + 0.1(\dot{q}_d(\tau) - r + \alpha e)$. The mode of the human-rider system is determined by the advanced crank angle using $H_1 \triangleq h_1(e, r, \tau) \bmod 2\pi$. Let $h_2 : \mathbb{R}^2 \times \mathbb{R}_{\geq t_0} \to \mathcal{P}$ denote the mode of the human-rider system, such that, for $\ell \in \{1, 2, \ldots, \mathtt{P} - 1\}$, $h_2(e, r, \tau) = \ell$ if and only if $H_1 \in [q_\ell, q_{\ell+1})$. For $\ell = \mathtt{P}$, let $h_2(e, r, \tau) = \mathtt{P}$ if and only if $H_1 \in [q_{\mathtt{P}}, q_1)$. The modulo operation of H_1 ensures the advanced angle $h_1(e, r, \tau)$ remains within $\mathcal{Q}$ for all $(e, r, \tau) \in \mathbb{R}^2 \times \mathbb{R}_{\geq t_0}$. In addition, whenever $H_1 \notin \mathcal{Q}^*$, one has that $\dot{p} = 0$. Substituting (2), (3), and (12) into the time derivative of (7) yields $\dot{r} = \Psi_h(e, r, \tau)$, where

$$\Psi_h\Big(e, r, \tau, \tau_{\int}\Big) \triangleq M_h^{-1}(e, \tau) \cdot (S_h(e, r, \tau) - H_h(e, r, \tau) r - \tau_{int} - B_p \text{sat}_{U_h}(k_1 r), \tag{14}$$

and $S_h : \mathbb{R}^2 \times \mathbb{R}_{\geq t_0} \to \mathbb{R}$ is a known function that is respectively defined and bounded as $S_h \triangleq M_h \ddot{q}_d + H_h(\dot{q}_d + \alpha e) + G_h + P + M_h \alpha \dot{e}$ and $|S_h| \leq c_1 + c_2\|z\| + c_3\|z\|^2$ using

Property 1. Additionally, recall that $H_h(e, r, \tau)$ is a known function that can be bounded according to Property 1. Let $\xi_h \triangleq [z^\top, \tau, p]^\top \in \mathcal{X}_h$ and $\mathcal{X}_h \triangleq \mathbb{R}^2 \times \mathbb{R}_{\geq t_0} \times \mathcal{P}$ denote the state and state space of the human-rider hybrid system $\mathcal{H}_h$, respectively. Recall that the interaction torque τ_{int} in (2) acts as an input for the human-rider system. Hence, following [12], the flow set of $\mathcal{H}_h$ is $C_h \triangleq \mathcal{X}_h \times \mathbb{R}$. The flow map $f_h : \mathcal{X}_h \times \mathbb{R} \to \mathcal{X}_h$ is obtained by using (7), (14), $\dot{\tau} = 1$, and $\dot{p} = 0$, such that

$$f_h(\xi_h, \tau_{int}) \triangleq [r - \alpha e, \Psi_h(e, r, \tau, \tau_{int}), 1, 0]^\top. \tag{15}$$

The jump set of $\mathcal{H}_h$ is $D_h \triangleq \{(\xi_h, \tau_{int}) \in \mathcal{X}_h \times \mathbb{R} : H_1 \in Q^*\}$, i.e., the hybrid system $\mathcal{H}_h$ exhibits a jump whenever the advanced crank angle transitions between different muscle effectiveness regions. Since e, r, and τ are continuous-time systems, $e^+ = e$, $r^+ = r$, and $\tau^+ = \tau$ whenever a jump occurs. Nevertheless, the mode index of the human-rider system is updated according to $p^+ = h_2(e, r, \tau)$. Using these difference equations, the jump map $g_h : \mathcal{X}_h \times \mathbb{R} \to \mathcal{X}_h$ of $\mathcal{H}_h$ is

$$g_h(\xi_h, \tau_{int}) \triangleq [e, r, \tau, h_2(e, r, \tau)]^\top. \tag{16}$$

Given the hybrid system $\mathcal{H}_h$ with data (C_h, f_h, D_h, g_h), the set of interest is $\mathcal{A}_h \triangleq \{(\xi_h, \tau_{int}) \in \mathcal{X}_h \times \mathbb{R} : z = \mathbf{0}\}$.

E. Motorized Cycle Hybrid System

Recall, the cycle is tasked with tracking an admitted position and cadence. By substituting (4), (5), and (13) into the time derivative of (9), one has that $\dot{\psi} = \Psi_r(\upsilon, \psi, \tau)$, where

$$\begin{aligned}\Psi_r(\upsilon, \psi, \tau) \triangleq M_r^{-1}(\upsilon, \tau) \cdot (S_r(\upsilon, \psi, \tau) - H_r(\upsilon, \psi, \tau)\psi \\ - k_2\psi - \nu \cdot \operatorname{sgn}(\psi) - (1 + \exp(-\tau))\upsilon),\end{aligned} \tag{17}$$

and $S_r : \mathbb{R}^2 \times \mathbb{R}_{\geq 0} \to \mathbb{R}$ is a known function respectively defined and bounded as $S_r \triangleq M_r(\ddot{q}_a + \ddot{q}_d) + H_r(\dot{q}_a + \dot{q}_d + \beta\upsilon) + G_r + b\dot{q} + M_r\beta\dot{\upsilon}$ and $|S_r| \leq c_4 + c_5\|\gamma\| + c_6\|\gamma\|^2$ using Property 1. Compared to [6], [7], the absence of an exogenous disturbance leads to a smaller bounding constant c_4, and therefore, a smaller sliding-mode gain. Similarly, $H_r(e, r, \tau)$ is a known function that can be bounded according to Property 1. Let $\xi_r \triangleq [\zeta^\top, \tau]^\top \in \mathcal{X}_r$ and $\mathcal{X}_r \triangleq \mathbb{R}^2 \times \mathbb{R}_{\geq t_0}$ denote the state and state space of the hybrid system for the motorized cycle, respectively, which is represented by $\mathcal{H}_r$. The flow set of $\mathcal{H}_r$ is $C_r \triangleq \mathcal{X}_r \times \mathbb{R}$, where τ_{int} in (4) acts as an input for the motorized cycle system. Using (9), (17), and $\dot{\tau} = 1$, the flow map f_r:$\mathcal{X}_r \times \mathbb{R} \to \mathcal{X}_r$ is

$$f_r(\xi_r, \tau_{int}) \triangleq [\psi - \beta\upsilon, \Psi_r(\upsilon, \psi, \tau), 1]^\top. \tag{18}$$

Since each function in ξ_r is continuous, the jump set of $\mathcal{H}_r$ is $D_r \triangleq \varnothing$ with a jump map $g_r : \mathcal{X}_r \times \mathbb{R} \to \mathcal{X}_r$ specified by

$$g_r(\xi_r, \tau_{int}) \triangleq [\upsilon, \psi, \tau]^\top. \tag{19}$$

Given the hybrid system $\mathcal{H}_r$ with data (C_r, f_r, D_r, g_r), the set to stabilize is $\mathcal{A}_r \triangleq \{(\xi_r, \tau_{int}) \in \mathcal{X}_r \times \mathbb{R} : \zeta = \mathbf{0}\}$, where the distance of ξ_r to $\mathcal{A}_r$ is characterized by $|\xi_r|_{\mathcal{A}_r} \triangleq \|\zeta\|$.

V. Stability Analysis

Theorem 1 shows the cycle's motor successfully regulates the interaction torque according to the filter dynamics in (11). Theorem 2 shows that the rider is stimulated when the cycle's cadence is below the desired cadence, i.e., while a torque error exists. Theorems 2 and 3 prove that the cadence and admittance controllers are bounded, i.e., $u_h, u_r \in \mathcal{L}_\infty$. While there is no guarantee of torque regulation, Theorems 1–3 guarantee emulation of the dynamics in (11) with bounded cadence and controllers. To facilitate the analysis, let $V_r : \mathcal{X}_r \to \mathbb{R}$ denote a candidate Lyapunov function given by

$$V_r(\xi_r) \triangleq \tfrac{1}{2}M_r\psi^2 + \tfrac{1}{2}(1 + \exp(-\tau))\upsilon^2, \tag{20}$$

which can be bounded by Property 1 as

$$\lambda_1|\xi_r|_{\mathcal{A}_r}^2 \leq V_r(\xi_r) \leq \lambda_2|\xi_r|_{\mathcal{A}_r}^2, \tag{21}$$

where $\lambda_1 \triangleq \frac{1}{2}\min(c_{m_r}, 1) \in \mathbb{R}_{>0}$ and $\lambda_2 \triangleq \max(\frac{1}{2}c_{M_r}, 1) \in \mathbb{R}_{>0}$. Furthermore, let $V_h : \mathcal{X}_h \to \mathbb{R}$ and $V_a : \mathbb{R} \to \mathbb{R}$ denote positive-definite storage functions given by

$$V_h(\xi_h) \triangleq \tfrac{1}{2}M_h \exp(-p)r^2 + \tfrac{1}{2}\exp(-\tau)e^2, \tag{22}$$

$$V_a(\dot{q}_a) \triangleq \tfrac{1}{2}M_d\dot{q}_a^2. \tag{23}$$

Theorem 1: The set $\mathcal{A}_r$ is globally exponentially stable for the hybrid system $\mathcal{H}_r$ with data (C_r, f_r, D_r, g_r) if the gains in (13) are selected according to the following sufficient conditions: $k_2 > 0$, $k_3 \geq c_4$, $k_4 \geq c_5$, and $k_5 \geq c_6$.

Proof: Consider the Krasovskii regularization of the flow map provided in (18), which is given by

$$\begin{aligned}F_r^r(\xi_r, \tau_{int}) &\triangleq \left[\psi - \beta\upsilon, \Psi_r^r(\upsilon, \psi, \tau), 1\right]^\top, \\ \Psi_r^r(\upsilon, \psi, \tau) &\triangleq \Big\{M_r^{-1} \cdot \Big[S_r - H_r\psi - k_2\psi \\ &\quad - (1 + \exp(-\tau))\upsilon - \nu \cdot \operatorname{SGN}(\psi)\Big].\end{aligned} \tag{24}$$

Let $\operatorname{SGN}(\psi) \triangleq \overline{\text{con}}\{\text{sgn}(\psi)\}$, where $\operatorname{SGN}(\psi) \triangleq 1$ for $\psi > 0$, $\operatorname{SGN}(\psi) \triangleq [-1, 1]$ for $\psi = 0$, and $\operatorname{SGN}(\psi) \triangleq -1$ for $\psi < 0$.[2] During flows, the change in V_r is given by $\langle \nabla V_r(\xi_r), \eta \rangle$ whenever $(\xi_r, \tau_{int}) \in C_r$ and $\eta \in F_r^r(\xi_r, \tau_{int})$.

Case I ($\psi > 0$): After employing (18) and utilizing Property 2, one has that

$$\begin{aligned}\langle \nabla V_r(\xi_r, \tau_{int}), \eta \rangle &= \psi S_r - k_2\psi^2 - \psi\nu - \beta\upsilon^2 \\ &\quad - (1/2 + \beta)\exp(-\tau)\upsilon^2 \\ &\leq -k_2\psi^2 - \beta\upsilon^2.\end{aligned} \tag{25}$$

Case II ($\psi = 0$): The change in (20) is

$$\begin{aligned}\langle \nabla V_r(\xi_r, \tau_{int}), \eta \rangle &= -\beta\upsilon^2 - (1/2 + \beta)\exp(-\tau)\upsilon^2 \\ &\leq -\beta\upsilon^2 = -k_2\psi^2 - \beta\upsilon^2.\end{aligned} \tag{26}$$

Case III ($\psi < 0$): The change in (20) is

$$\begin{aligned}\langle \nabla V_r(\xi_r, \tau_{int}), \eta \rangle &= \psi S_r - k_2\psi^2 + \psi\nu - \beta\upsilon^2 \\ &\quad - (1/2 + \beta)\exp(-\tau)\upsilon^2 \\ &\leq -k_2\psi^2 - \beta\upsilon^2.\end{aligned} \tag{27}$$

Hence, for $\psi \in \mathbb{R}$, $\langle \nabla V_r(\xi_r, \tau_{int}), \eta \rangle \leq -k_2\psi^2 - \beta\upsilon^2$, where (21) and $\lambda_3 \triangleq \min(k_2, \beta) \in \mathbb{R}_{>0}$ yield

$$\langle \nabla V(\xi_r, \tau_{int}), \eta \rangle \leq -\lambda_3|\xi_r|_{\mathcal{A}}^2 \leq -\tfrac{\lambda_3}{\lambda_2}V_r(\xi_r). \tag{28}$$

[2]The set-valued mapping $\operatorname{SGN}(\psi)$ is outer semicontinuous and locally bounded for every $\psi \in \mathbb{R}$.

Since $D_r = \varnothing$, $V_r(\xi_r)$ exhibits no jumps and $j = 0$ for all $t \geq 0$. Given a complete solution $\phi(t, j)$, integrating (28) yields[3]

$$V_r(\phi(t,j)) \leq \exp\Big(-\tfrac{\lambda_3}{\lambda_2} t\Big) V_r(\phi(0,0)). \tag{29}$$

Using this fact, and substituting (21) into (29), we see that $\mathcal{A}_r$ is GES with respect to Definition 1 since

$$|\phi(t,j)|_{\mathcal{A}_r} \leq \kappa_{1,r} \exp\big(-\kappa_{2,r}(t+j)\big) |\phi(0,0)|_{\mathcal{A}_r}, \tag{30}$$

where $\kappa_{1,r} \triangleq \sqrt{\lambda_2/\lambda_1}$ and $\kappa_{2,r} \triangleq \lambda_3/(2\lambda_2)$. By (30), $\phi(t,j) \in \mathcal{L}_\infty$, for all $(t,j) \in \text{dom}\phi$, which implies $\upsilon, \psi \in \mathcal{L}_\infty$. ■

Remark 1: The hybrid system $\mathcal{H}_r$ satisfies the hybrid basic conditions [11, Assumption 6.5]. Moreover, since $\mathcal{A}_r$ is GES, it can be shown that $\mathcal{A}_r$ is robust to vanishing perturbations [11, Lemma 7.20]. This is beneficial in human-robot interaction because the human may apply involuntary disturbances to the system, especially during stimulation, e.g., reflexes, spasms, and volitional contributions. Under a persistent disturbance, solutions of $\mathcal{H}_r$ are uniformly ultimately bounded, where the ultimate bound is a function of the gains.

Theorem 2: Let $k_1 > 0$. The hybrid system $\mathcal{H}_h$ with data (C_h, f_h, D_h, g_h) is output feedback passive relative to $\mathcal{A}_h$ with flow input $u_c \triangleq |\tau_{int}|$, jump input $u_d \triangleq 0$, and the flow/jump output $y_c = y_d \triangleq \|z\|$. Recall that $z = [e, r]^\top$.

Proof: During flows, the change in V_h is given by $\langle \nabla V_h(\xi_h), f_h(\xi_h, \tau_{int}) \rangle$ for each $(\xi_h, \tau_{int}) \in C_h$. Hence, after employing (15) and utilizing Property 2, it follows that

$$\begin{aligned}\langle \nabla V_h(\xi_h), f_h(\xi_h, \tau_{int}) \rangle &= \exp(-p) r \big(S_h - B_p \text{sat}_{U_h}[k_1 r] - \tau_{int}\big) \\ &+ \exp(-\tau) e (r - \alpha e) - \tfrac{1}{2} \exp(-\tau) e^2. \end{aligned} \tag{31}$$

Observe that (31) can be upper bounded with $B_p = 0$ for all $q^* \in \mathcal{Q}$, which yields

$$\begin{aligned}\langle \nabla V_h(\xi_h), f_h(\xi_h, \tau_{int}) \rangle &\leq |r||S_h| + |\tau_{int}||r| + |e||r| \\ &\leq u_c y_c + y_c \rho_c(y_c), \end{aligned} \tag{32}$$

where V_h in (22) is the storage function, and ρ_c denotes a known, positive definite, radially unbounded function. During jumps, the change in V_h is given by $V(g) - V(\xi_h, \tau_{int})$ for $(\xi_h, \tau_{int}) \in D_h$ and $g = g_h(\xi_h, \tau_{int})$, where (16) implies

$$V_h(g) - V_h(\xi_h, \tau_{int}) = \tfrac{1}{2} M_h \left(\frac{1}{\exp(h_2)} - \frac{1}{\exp(p)} \right) r^2. \tag{33}$$

Using Property 1 and (7), (33) can be upper bounded as

$$V_h(g) - V_h(\xi_h, \tau_{int}) \leq u_d y_d + y_d \rho_d(y_d), \tag{34}$$

where the jump input is $u_d \equiv 0$, the jump output is $y_d = \|z\|$, and ρ_d denotes a known, positive definite, radially unbounded function. Definition 2 can be used with (32) and (34) to show that the hybrid system $\mathcal{H}_h$ is output feedback passive with respect to $\mathcal{A}_h$. Because regulating the solutions of $\mathcal{H}_h$ to $\mathcal{A}_h$ is not the primary objective, this shortage of passivity does not prevent the solutions of $\mathcal{H}_r$ from converging to $\mathcal{A}_r$. Due to the saturation function in (12), the cadence controller (i.e., stimulation) is bounded by construction, i.e., $u_h \in \mathcal{L}_\infty$. ■

[3]Formally, completeness of solutions must be shown. To do so, one method is to employ [11, Proposition 2.10]. However, we reserve this task for future work given the limited space and the complex nonlinear behavior of the flow dynamics in (17)-(18).

Theorem 3: The admittance filter in (11) is output strictly passive (see [17, Definition 6.3]) for all $t \geq t_0$ with input $u \triangleq e_\tau$, output $y \triangleq \dot{q}_a$, and storage function V_a defined in (23) provided the filter parameters are selected according to the following sufficient conditions: $M_d > 0$ and $B_d > 0$.

Proof: Taking the time derivative of (23) and substituting (11) yields $\dot{V}_a = e_\tau \dot{q}_a - B_d \dot{q}_a^2 = uy - y\rho(y)$, which proves the admittance filter in (11) is output strictly passive (OSP) with input u, output y, and storage function V_a. Recall that $\tau_{int} \in \mathcal{L}_\infty$ [19], and $\upsilon, \psi \in \mathcal{L}_\infty$ by Theorem 1. Because (11) is OSP, $\tau_{int} \in \mathcal{L}_\infty$ implies $\dot{q}_a, \ddot{q}_a \in \mathcal{L}_\infty$. Next, $\upsilon, \psi, \dot{q}_a, \ddot{q}_a \in \mathcal{L}_\infty$ implies $\gamma \in \mathcal{L}_\infty$. Hence, (13) implies the admittance controller (i.e., motor current) is bounded, i.e., $u_r \in \mathcal{L}_\infty$, since $\upsilon, \psi, \gamma, \tau_{int} \in \mathcal{L}_\infty$. ■

VI. Experiments

A. Experimental Testbed

Experiments are conducted using a modified recumbent cycle (Terratrike). The angular position and velocity of the cycle's crank are measured with a U.S. Digital H5-5000-IE-S encoder. The interaction torque is measured with an SRM Science Road powermeter. The cycle uses a 350-Watt DC motor and is controlled with an AMC servo drive. The sensors and motor use a Quanser data acquisition board with a Windows 10 computer. All control algorithms are implemented in MATLAB and SIMULINK. To prevent ankle flexion and maintain sagittal alignment of the rider's legs, the rider's feet are attached to the cycle's pedals with orthotic boots. The rider's muscles are stimulated with a Hasomed RehaStim3 electrical stimulator delivering symmetric, biphasic, and rectangular pulses with bipolar self-adhesive PALS electrodes. For simplicity, only the rider's quadriceps and hamstrings muscles were stimulated. Stimulation was applied at a frequency of 60 Hz and current amplitudes of 90 mA and 70 mA for the quadriceps and hamstrings, respectively. Emergency stops and staff were available to the rider at all times. Additional details on the testbed are available in [7].

B. Experimental Methods

To verify the efficacy of the proposed approach, 4-minute experiments were carried out on five participants, aged 20-29, four males and one female, without any neurological injuries. For the first 30 seconds of each experiment, only the cycle's motor is used to bring the cycle to the desired cadence of 50 RPM; afterward, stimulation was applied. All participants are blind to their performance and instructed to relax and make no voluntary effort to assist or resist the cycle. For all experiments, the controller gains in (6), (9), (12), and (13) were selected as $k_1 = k_2 = 4$, $k_3 = 0.1$, $k_4 = k_5 = 0.01$, $\alpha \in [0.8, 1]$, $\beta = 1$. While the aforementioned gain conditions in Theorem 1 are sufficient to achieve stability based on conservative bounds on the uncertain parameters in the dynamics, they are sufficient, but not necessary. Therefore, the sufficient gain conditions provide guidelines for the initial gain selection and the gains were subsequently adjusted to achieve desirable performance. In (11), the parameters were set as $M_d = 10 \frac{\text{N·m·s}^2}{\text{rad}}$, $B_d = 2 \frac{\text{N·m·s}}{\text{rad}}$, and $\tau_d \in [-0.25, 0]\,\text{N·m}$.[4]

[4]Note, a negative τ_d still requires the rider to exert a positive torque about the crank as long as τ_d is greater than the torque it takes to passively move the rider's legs; τ_d was selected and tuned based on the rider's performance.

TABLE I
EXPERIMENTAL RESULTS

Participant	$\dot{q}$ (RPM)	$\dot{e}$ (RPM)	$\dot{v}$ (RPM)
P1	44.11 ± 2.18	5.89 ± 2.18	-0.01 ± 0.46
P2	47.53 ± 1.71	2.47 ± 1.71	-0.01 ± 0.65
P3	43.55 ± 1.74	6.45 ± 1.74	-0.02 ± 0.60
P4	43.69 ± 2.38	6.31 ± 2.38	-0.02 ± 1.18
P5	48.69 ± 0.84	1.31 ± 0.84	-0.01 ± 0.59
Mean	45.51 ± 1.77	4.49 ± 1.77	-0.01 ± 0.70

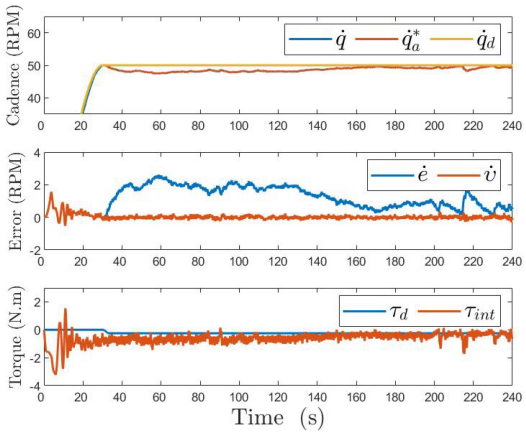

Fig. 1. Participant P5. (Top) Cadence tracking results showing the measured cadence $\dot{q}$, admitted cadence $\dot{q}_a^* \triangleq \dot{q}_d + \dot{q}_a$, and desired cadence $\dot{q}_d$. (Middle) Cadence tracking error $\dot{e}$, and admitted cadence tracking error $\dot{v}$. (Bottom) The desired interaction torque τ_d, and the interaction torque τ_{int}. For visual clarity, a 1-second moving average filter was applied to the plots.

All experimental procedures were approved by the University of Alabama under IRB Protocol #20-005-ME.

C. Results and Discussion

Figure 1 displays the tracking results for Participant P5. The rider's stimulation increases over the course of the experiment until it reaches saturation at time $t \approx 220$ s. As the stimulation increases, the rider's muscles produce an increasing amount of interaction torque, and cause convergence of the cadence error system, as shown in Figure 1. When the rider produces the desired amount of torque, τ_{int} aligns with τ_d, the admitted cadence tends toward the desired cadence, and both cadence error systems converge toward zero. At time $t \approx 170$ s, the rider starts to fatigue leading to an increase in stimulation to maintain constant interaction torque (not shown). In contrast to the admittance error system–which is held near zero over the experiment–as the rider's stimulation is saturated, the cadence error degrades due to insufficient actuation. Observe that at time $t \approx 225$ s, the cadence tracking error sharply increases and subsequently decreases; we surmise this is an indication of the rider's volitional contribution to cycling.

VII. CONCLUSION

Two tracking objectives are presented for a motorized FES cycle. A cadence tracking objective is assigned to the rider, whose muscles are activated via FES, and using a hybrid passivity-based analysis, it is shown that the closed-loop cadence hybrid system is output feedback passive with respect to the origin. Simultaneously, the cycle's motor is tasked with indirectly tracking a desired torque using an admittance controller. Using a hybrid Lyapunov-based analysis, it is shown that the origin is globally exponentially stable. Experiments are conducted to validate the efficacy of the proposed approach. Future works will incorporate additional operating modes to the FES cycle, an in-depth analysis of fatigue, and an expanded joint Lyapunov-passivity analysis for hybrid systems.

REFERENCES

[1] "Spinal cord injury facts and figures at a glance," Data Sheet, Nat. SCI Stat. Center, Birmingham, AL, USA, 2020.
[2] V. L. Feigin *et al.*, "Burden of neurological disorders across the US from 1990-2017: A global burden of disease study," *JAMA Neurol.*, vol. 78, no. 2, pp. 165–176, 2021.
[3] N. H. Mayer, "Clinicophysiologic concepts of spasticity and motor dysfunction in adults with an upper motoneuron lesion," *Muscle Nerve*, vol. 20, no. S6, pp. 1–14, 1997.
[4] L. R. Sheffler and J. Chae, "Neuromuscular electrical stimulation in neurorehabilitation." *Muscle Nerve*, vol. 35, no. 5, pp. 562–590, May 2007.
[5] R. Berkelmans, "FES cycling," *J. Autom. Control*, vol. 18, no. 2, pp. 73–76, 2008.
[6] C. A. Cousin *et al.*, "Closed-loop cadence and instantaneous power control on a motorized functional electrical stimulation cycle," *IEEE Trans. Control Syst. Technol.*, vol. 28, no. 6, pp. 2276–2291, Nov. 2020.
[7] C. A. Cousin, C. A. Rouse, V. H. Duenas, and W. E. Dixon, "Controlling the cadence and admittance of a functional electrical stimulation cycle," *IEEE Trans. Neural Syst. Rehabil. Eng.*, vol. 27, no. 6, pp. 1181–1192, Jun. 2019.
[8] J. Aldrich and C. A. Cousin, "Smoothly switched adaptive torque tracking for functional electrical stimulation cycling," *IEEE Control Syst. Lett.*, vol. 6, pp. 866–871, Jun. 2021, doi: 10.1109/LCSYS.2021.3086772.
[9] S. Akbari, G. Merritt, and C. A. Cousin, "Electromyography-based cadence control of functional electrical stimulation cycle," in *Proc. RehabWeek*, 2021, pp. 189–192.
[10] A. R. Teel, F. Forni, and L. Zaccarian, "Lyapunov-based sufficient conditions for exponential stability in hybrid systems," *IEEE Trans. Autom. Control*, vol. 58, no. 6, pp. 1591–1596, Jun. 2013.
[11] R. G. Goebel, R. Sanfelice, and A. R. Teel, *Hybrid Dynamical Systems*. Princeton, NJ, USA: Princeton Univ.Press, 2012.
[12] R. Naldi and R. G. Sanfelice, "Passivity-based control for hybrid systems with applications to mechanical systems exhibiting impacts," *Automatica*, vol. 49, no. 5, pp. 1104–1116, 2013.
[13] A. R. Teel, A. Subbaraman, and A. Sferlazza, "Stability analysis for stochastic hybrid systems: A survey," *Automatica*, vol. 50, no. 10, pp. 2435–2456, 2014.
[14] F. Sado, S. N. Sidek, and H. M. Yusof, "Adaptive hybrid impedance control for a 3DOF upper limb rehabilitation robot using hybrid automata," in *Proc. IECBES*, 2014, pp. 596–601.
[15] V. B. Semwal, S. A. Katiyar, R. Chakraborty, and G. C. Nandi, "Biologically-inspired push recovery capable bipedal locomotion modeling through hybrid automata," *Robot. Auton. Syst.*, vol. 70, pp. 181–190, Aug. 2015.
[16] F. M. Zegers, S. Phillips, and W. E. Dixon, "Consensus over clustered networks with asynchronous inter-cluster communication," in *Proc. Amer. Control Conf.*, 2021, pp. 4249–4254.
[17] H. K. Khalil, *Nonlinear Systems*, 3rd ed. Upper Saddle River, NJ, USA: Prentice Hall, 2002.
[18] M. J. Bellman, R. J. Downey, A. Parikh, and W. E. Dixon, "Automatic control of cycling induced by functional electrical stimulation with electric motor assistance," *IEEE Trans. Autom. Sci. Eng.*, vol. 14, no. 2, pp. 1225–1234, Apr. 2017.
[19] Y. Li and S. S. Ge, "Impedance learning for robots interacting with unknown environments," *IEEE Trans. Control Syst. Technol.*, vol. 22, no. 4, pp. 1422–1432, Jul. 2014.
[20] A. Behal, W. E. Dixon, B. Xian, and D. M. Dawson, *Lyapunov-Based Control of Robotic Systems*. Boca Raton, FL, USA: Taylor and Francis, 2009.
[21] R. Downey, M. Merad, E. Gonzalez, and W. E. Dixon, "The time-varying nature of electromechanical delay and muscle control effectiveness in response to stimulation-induced fatigue," *IEEE Trans. Neural Syst. Rehabil. Eng.*, vol. 25, no. 9, pp. 1397–1408, Sep. 2017.